Space Science Reviews (2023) 219:78
https://doi.org/10.1007/s11214-023-01023-4

Tunable Laser Spectrometers for Planetary Science

Christopher R. Webster[1] · Amy E. Hofmann[1] · Paul R. Mahaffy[2] · Sushil K. Atreya[3] · Christopher H. House[4] · Amy A. Simon[2] · James B. Garvin[2]

Received: 1 June 2023 / Accepted: 3 November 2023

Abstract

Distinguishing planetary formation and evolution pathways and understanding the origins of volatiles on planetary bodies requires determination of relative abundances and isotope ratios in the noble gases, and also of the isotope ratios in C, H, N, O and S at high precisions. Traditional planetary mass spectrometers uniquely provide excellent survey capability including the noble gas relative abundances and their isotope ratios. However, to distinguish planetary evolution models for the outer planets, stable isotope ratios in C and O require precisions of ∼10‰ or better, readily achievable with a tunable laser spectrometer (TLS). As demonstrated on the Mars Curiosity rover, and as planned for a now-selected NASA Venus mission, tunable laser spectrometers play a unique role synergistic with the capabilities of planetary mass spectrometers. The TLS technique of recording infrared absorption spectra at ultrahigh resolution (resolving power $\lambda/\delta\lambda \sim 5$ million) provides unambiguous detection of a wide variety of gases such as H_2O, H_2O_2, H_2CO, HOCl, NO, NO_2, HNO_3, N_2O, O_3, CO, CO_2, NH_3, N_2H_4, PH_3, H_2S, SO_2, OCS, HCl, HF, O_2, HCN, and CH_4, C_2H_2, C_2H_4, C_2H_6 at parts-per-billion levels. Through line-depth or line-area ratio comparisons of adjacent spectral lines, planetary TLS instruments can achieve isotope ratio measurements in C, H, N, O, and S molecules at precisions of ∼1–2‰, including for the triple isotope components of O and S. Expected performance of TLS instruments for Venus, Saturn, Enceladus and Uranus will be described as constrained by actual measurements reported at Mars on the Curiosity rover.

Keywords Planetary · Laser · Isotope ratios · Spectrometer

✉ C.R. Webster
Chris.R.Webster@jpl.nasa.gov

1 Jet Propulsion Laboratory, California Institute of Technology, Pasadena, CA, USA

2 NASA Goddard Space Flight Center, Greenbelt, MD, USA

3 University of Michigan, Ann Arbor, MI, USA

4 Pennsylvania State University, University Park, PA, USA

Published online: 22 November 2023

1 Introduction

1.1 Science Drivers

The foundation of our understanding of the origin and evolution of solar system bodies is through comparative planetology that establishes the differing bulk, atmospheric and surface compositions. This is achieved through comparison of values for individual planets with those of the Sun, comets and meteorites. While cometary composition establishes chemical composition during formation of the solar system, for other solar system bodies, isotope ratios in the noble gases and in C, H, N, O and S can reveal not only the primordial form of volatiles, but also their temperature and reaction history (Mandt et al. 2015) that may suggest earlier planetary migration. From ground-based observations and from numerous planetary missions to date, the large but incomplete data base is created from measurements using two primary techniques: mass and optical spectroscopy, that can distinguish atomic and molecular components through unambiguous signatures in either absolute mass or in fingerprint spectral lines (from ultraviolet to radio frequencies) seen in absorption or emission. Both these techniques have been used to date in remote sensing (at-distance, on-orbit, or flyby) and in situ sensing at lower altitudes using atmospheric probes or at-surface landers and rovers. For the latter, gas samples may be near-surface atmospheric, evolved from heating surface materials, or returned to Earth for analysis.

Following the formation of planetesimals through accretion, those closer to the Sun at higher temperatures are expected to have been depleted in volatiles, while those beyond ~4 astronomical units (AU) retained significant abundances of water ice and other volatiles (Mandt et al. 2015). Current understanding indicates that after formation, the inner planets (e.g. Mercury, Venus, Earth, Mars) migrated toward the Sun, while the gas and ice giants (Jupiter, Saturn, Uranus and Neptune) migrated outwards to varying extent. Comets are thought to have originated primarily in the Oort Cloud some 5–30 AU from the Sun, and Jupiter Family Comets (JFC) in the Kuiper Belt at 30–35 AU (see review by Dones et al. 2015).

The goal of planetary science is to understand the formation, migration and current composition of solar system bodies that is consistent with the sometimes-complex processes associated with volatile acquisition, exchange and temperature history. In a sense, it's reverse-engineering from current-day compositions to extrapolate over a very long time period back to formation.

The readily-accessible terrestrial planets Venus, Earth and Mars have been extensively studied, but that is not true for the gas and ice giants. Once more, comparative planetology is key to unraveling the mystery of the origin and evolution of the giant planets in particular, and the solar system in general. While Jupiter and Saturn have been studied by various space-borne and ground-based assets including Juno, Galileo and Cassini, only rudimentary data from the Voyager flybys and the earth are available for Uranus and Neptune. The abundance and the isotopic ratios of key heavy elements, C, N, S and O, and the noble gases He, Ar, Kr, Xe and Ne provide the best constraints for the giant planet formation models but they are largely missing for the ice giants (Atreya et al. 2020). Noble gases are expected to be well mixed below the homopause, but they can only be measured in situ with a mass spectrometer on an entry probe at relatively shallow atmospheric pressure level of one to a few bars like the Galileo Probe at Jupiter (Niemann et al. 1998; Mahaffy et al. 2000).

The elemental abundance of C, N, S and O in the giant planets can be determined from their bulk reservoirs, CH_4, NH_3, H_2S and H_2O, again like the Galileo probe at Jupiter, but it requires accessing the well-mixed atmosphere, which lies below the condensation level

for each of the condensable gases. That is especially challenging at the icy giants whose cold temperatures push the condensation levels very deep into the atmosphere as illustrated in Fig. 1 of Atreya et al. (2020). According to thermochemical equilibrium models with 45 times solar abundance of CH_4 and solar abundance for the other condensables, the cloud bases of CH_4, NH_3, NH_4SH and H_2O would be at approximately 1.5, 10, 30 and 90 bars, respectively (Fig. 5 of Atreya et al. 2020) at Uranus and Neptune, which have very similar temperature structures. In reality the bulk composition, which allows the determination of elemental abundances needed for formation models, may be much, much deeper than the predicted cloud bases, as was found for Jupiter with Juno (Bolton et al. 2017; Li et al. 2020). At Jupiter, models predict the cloud base of NH_3 at 0.7 bar and 8 bars for H_2O for 3 times solar abundance but Juno found that their well-mixed levels are well below the bases, at tens of bars and possibly much deeper.

Microwave remote sensing could in principle allow the measurement of NH_3 and H_2O bulk abundance if it can remove the degeneracy in brightness temperature, NH_3 and H_2O, but that is not a given for the icy giants. The Very Large Array (VLA) observations of Uranus and Neptune showed that NH_3 is depleted by a factor of 100–1000 relative to its solar abundance (de Pater et al. 1989, 1991) and H_2O is not detected. The depletion in NH_3 is attributed to possible loss in an ammonium hydrosulfide cloud at tens of bars and/or an anionic/superionic ocean at 100's of kilobars (Atreya et al. 2020). The VLA data correspond to only 10–30 bars, which is likely not deep enough for finding the bulk abundance of ammonia. Entry probe measurements at Uranus will be limited to about 10 bars or so also, but that may not be deep enough for CH_4 either to reach its well-mixed level, even though its predicted cloud base is at $\sim$1.5 bars. Thus, the main focus of TLS on a Uranus probe is precision isotope measurements and gradients in density profiles of CH_4, NH_3, H_2S and H_2O, whichever are encountered, rather than their bulk abundance. On the other hand, the probe mass spectrometer will make the measurement of the elemental abundances and the isotopic ratios of the noble gases. A comparison of the isotopic ratios of stable gases and the noble gases in the icy giants with those available for the gas giants and other solar system bodies will reveal much about the processes that formed and shaped the icy giants into their present state.

1.2 In Situ Instrumentation

Mass spectrometers have played a key role over the past decades with in situ measurements to identify the chemical and isotopic composition of planetary targets (Arevalo et al. 2019). For example, investigations have targeted the atmosphere of Jupiter in 1995 with the Galileo Probe Mass Spectrometer (GPMS, Niemann et al. 1992), the deep and upper atmosphere of Venus with probes (Hoffman et al. 1980) and orbiters (Kasprzak et al. 1993), the atmosphere of Saturn's moon Titan from the Huygens probe (Niemann et al. 1997) and the Cassini Orbiter (Kasprzak et al. 2007), the coma of comets (Balsiger et al. 2007), the lunar exosphere (Mahaffy et al. 2014), and the atmosphere and surface of Mars (e.g. Mahaffy et al. 2015, 2012).

Noble gas and light element abundances and their isotopic composition support models of giant planet atmospheric formation (e.g. Atreya et al. 1999) and terrestrial planet evolution (e.g. Jakosky et al. 2017) while the in situ measurement of complex organic compounds will be critical in the search for biosignatures and life outside of Earth (Chou et al. 2021). Recent significant advances for planetary mass spectrometry include the development of linear ion trap mass spectrometers for the ExoMars Rosalind Franklin rover (Goetz et al. 2016) and the Dragonfly mission to Titan (Barnes et al. 2021; Trainer et al. 2018). These

instruments enable tandem mass spectrometry to fragment and elucidate the structure of complex molecules and sample either ionized molecules from a gas chromatograph or ions released from a solid surface using laser desorption (Li et al. 2017). In addition, the recent development of an ultra-high mass resolution ($m/\Delta m > 10^5$) orbitrap-based instrument for deep space use (Arevalo et al. 2023) is a significant technological advance toward the unambiguous identification of biogenic molecules such as amino acids and peptides that are of great interest for of life detection missions such as those planned (National Academies of Sciences, Engineering, and Medicine 2022) to Enceladus and Europa the ocean world moons of Saturn and Jupiter.

While orbitrap-based mass spectrometers or multi-bounce time of flight mass spectrometers (Brockwell et al. 2016) have the potential to resolve near-isobaric species, they remain less suitable for descent probe exploration of deep atmospheres due to their rigid vacuum requirements. On an airless ocean world body such as Europa or Enceladus, however, an orbitrap-based instrument could be an excellent choice for unambiguous identification, detection, and quantification of complex organics. Mass spectrometers on orbiters can be relatively large in size, but with size and mass constraints on atmospheric probes, planetary quadrupole mass spectrometers may be limited to unit mass resolution where they struggle to separate CO from N_2 at mass 28, to detect small molecules like H_2O, CH_4 and NH_3 in the lower mass region, and to untangle their various isotopic contributions at low mass numbers. Isobaric contributions may occur at mass 17 (e.g. NH_3, CH_3D, $^{13}CH_4$), mass 18 (e.g. H_2O, $^{15}NH_3$, NH_2D) and mass 19 (e.g. HDO, $H_2{}^{17}O$, $^{15}NH_2D$). Fragments of more complex hydrocarbon molecules may contribute to these mass channels as well, as suggested in analyses of Cassini INMS data from the Enceladus plume (Waite et al. 2017). The next-generation of high resolution ($m/\Delta m \sim 10^3$ to 10^4) mass spectrometers such as MASPEX, a multi-bounce TOF with a mass resolving power $m/\Delta m$ of $> 2 \times 10^4$ (Brockwell et al. 2016; Miller et al. 2021) to be flown on Europa Clipper, should be able to resolve many of these species, and thus demonstrates an enabling transition toward unambiguous identification and precise quantification of small volatile compounds and their isotopologues. However, these instruments in their current builds are unsuitably large for inclusion on atmospheric probes and in situ landers and rovers (Arevalo et al. 2019). With its ultrahigh spectral resolution and ability to select specific individual spectral lines, tunable laser spectrometers excel at detecting unambiguously these smaller molecules and resolving their isotopic components.

A great breadth of isotopic and chemical analysis can be provided by utilization of both a tunable laser spectrometer and a mass spectrometer as implemented on the Sample Analysis at Mars (SAM) experiment (Mahaffy et al. 2012) for the Mars Science Laboratory (MSL) and in development for the DAVINCI mission to Venus (Garvin et al. 2022) described later. The implementation of the two instruments into a suite provides efficiencies since sample processing from the atmosphere or of gases evolved from drilled rocks can be handled by a common system. While the mass spectrometer provides a general survey of all gases introduced into its ionization source, including the noble gases, the tunable laser spectrometer can provide isotope measurements for select C, H, N, O and S-bearing compounds at higher precision. The combination of a mass spectrometer and a tunable laser spectrometer thus provides the best possible instrumentation in a small package for gas abundances and isotopic ratios in either planetary atmospheres or in evolved gases derived from surface samples.

1.3 Measurement Requirements for Stable Isotope Ratios in C, H, N, O and S

Stable isotope ratios in C, H, N, O and S are powerful indicators of a wide variety of planetary geophysical processes (Miller et al. 2021). In specific compounds, such ratios can be

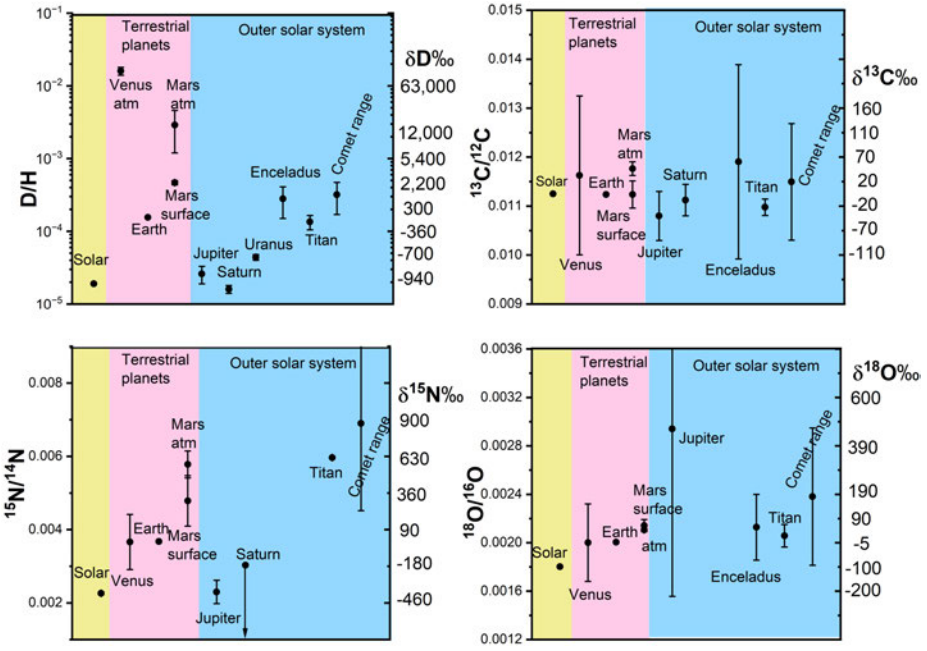

Fig. 1 Stable isotope ratio measurements in the solar system. Plots are modified after Fig. 10 of Hörst (2017) that contains numerical data and references. Additional Mars data points are from Curiosity (Leshin et al. 2013; Wong et al. 2013), and the D/H of Uranus is from Feuchtgruber et al. 2013. Rounded delta-values to the right of the plots are relative to Earth values, and those given for δD correspond to points 1, 2, and 5 on the logarithm scale

used to infer provenance, subsequent transport, last-equilibration temperature (and thus associated chemical and physical processes), radiation exposure of solar system bodies and their components (atmospheric species, hydrosphere, bulk mantle, etc.). This "forensic tracing" is especially true for surface or deep atmosphere samples that closely approximate the bulk composition of solid or gaseous planetary bodies. Complimentarily, the stable isotope values of planetary gases additionally reveal atmospheric escape and volatile loss. Together, the isotope ratios of C, H, N, O, and S can provide an integrated geochemical evaluation of the origin, evolution, and environmental habitability over time for a specific solar system body. In the case of the ancient Earth, Mars, and multiple ocean worlds, light stable isotopes are a central part of the search for evidence of biological processes (e.g. as summarized in Miller et al. 2021). In Fig. 1, modified after Hörst (2017), isotopic measurements made to date are plotted for terrestrial and outer solar system bodies for comparison with solar values. While many measurements are informative, we will argue that higher precision is needed for some ratios as future missions build upon the pioneering measurements of the past.

The D/H ratio in either H_2O or H_2 is regarded as one of the most fundamental planetary measurements, in part because of the need to understand if Earth's water was delivered by comet/asteroid combinations. Because the ground-state energies of either HD and H_2 or HDO and H_2O differ significantly due to the large relative mass difference between H and D, the magnitude of isotopic fractionation between H- and D-bearing isotopologues can be concomitantly larger, resulting in D/H ratios orders or magnitude higher than solar, as shown in Fig. 1. As such, the precision required on D/H ratios can be much less stringent than that for

other isotopic systems while still enabling discernment among, e.g., formation hypotheses. The D/H data set to date clearly distinguishes for example Jupiter and Saturn as solar, while measurements from Earth, Mars, Enceladus and Titan are currently within the wide range of cometary values. The Mars atmosphere in which escape processes enrich deuterium is clearly distinguished from range of values from surface materials. Baselining the Titan error bars as optimal for future measurements results in a desired precision of ~20% or better for D/H measurements. The D/H ratio of Uranus and Neptune are greater than those of Jupiter and Saturn, which are thought to represent the protosolar value. This difference is expected, considering that the icy/rocky component of the former could make up more than half their masses, unlike the gas giants, where solid components account for less than 10% of the planetary mass. The D/H value thus provides an important constraint on the ice/rock ratio for the formation models of Uranus and Neptune. Although D/H has been measured quite well from H_2 ($4.4 \pm 0.4 \times 10^{-5}$, Feuchtgruber et al. 2013) and CH_4 ($2.9\ (+0.9/-0.5) \times 10^{-4}$, Irwin et al. 2012) at Uranus, no measurements are available from H_2O. TLS measurement of D/H from CH_4 would also be important in confirming and refining the earlier results.

Isotope ratio measurements in nitrogen are sparse for the outer solar system, especially for the outer planets. Such measurements can provide insight into the primordial reservoir(s) of nitrogen (e.g. NH_3 ices versus N_2) incorporated into a given planetary body (Miller et al. 2021). The in-situ measurement of $^{15}N/^{14}N$ in Titan's near-surface atmospheric N_2 (Niemann et al. 2010) is within range of both cometary values (suggesting some contribution from N-bearing ices, although see spread represented by error bars in Fig. 1) and the Martian atmosphere, but is much higher (i.e. ^{15}N-enriched) than that of both Earth and of the protosolar value. The Jovian ratio of $(2.3 \pm 0.3) \times 10^{-3}$ as measured albeit with large error bars in ammonia (Owen et al. 2001) by the Galileo Probe Mass Spectrometer, and taken to be the average solar system value, was found to be much lower than that in terrestrial N_2, suggesting that the two bodies sourced their nitrogen from different materials. For Mars, the achieved measurement precision in the SAM QMS allows distinction between atmospheric (Wong et al. 2013) and surface reservoirs (Deligny et al. 2023). Ideally, future missions would allow determination of the $^{15}N/^{14}N$ ratio to precisions similar to that measured on Mars or Titan, namely to ~5% or for a $\delta^{15}N$ error of ~50‰.

As shown in Fig. 1, measured $^{13}C/^{12}C$ and $^{18}O/^{16}O$ ratios are all consistent with one another within error; therefore, higher precision analyses are required to ascertain whether and to what magnitude- these planetary bodies (and associated reservoirs) differ from one another in their carbon and oxygen isotopic composition. Apart from the Mars atmospheric and surface measurements, the errors on the $^{13}C/^{12}C$ ratios of all bodies are too large to show any distinction. Existing measurements at Venus, Enceladus (and even Jupiter to a lesser extent) are too imprecise to enable robust hypothesis testing. Ideally for future missions, the $^{13}C/^{12}C$ ratio needs to be measured to ~1%, representing a $\delta^{13}C$ error of ~10‰. The large error bars on $^{18}O/^{16}O$ ratios for compounds at Venus, Jupiter and Enceladus make those data indistinguishable from Earth's oceans or solar values. For future planetary missions, the $^{18}O/^{16}O$ ratio needs to be measured to precisions of ~1%, representing a $\delta^{18}O$ error of ~10‰, in order to compare the origins of volatiles in different planetary atmospheres or to identify processes at work on planetary surfaces and interactions between planetary surfaces and subsurface hydrospheres or the near-surface atmosphere.

Finally, triple isotopes ratios of O and S are important geochemical measurements in planetary science. Triple O isotopes are the principle tool for discerning the origin of planetary bodies because solar system materials appear to lie on a continuum between hypothetical highly ^{18}O- and ^{17}O-enriched water (Sakamoto et al. 2007) and the ^{16}O-rich protosun (McKeegan et al. 2011). Mass-independent processes, including atmospheric photochemical reactions, can produce large isotopic anomalies in oxygen and sulfur-bearing species

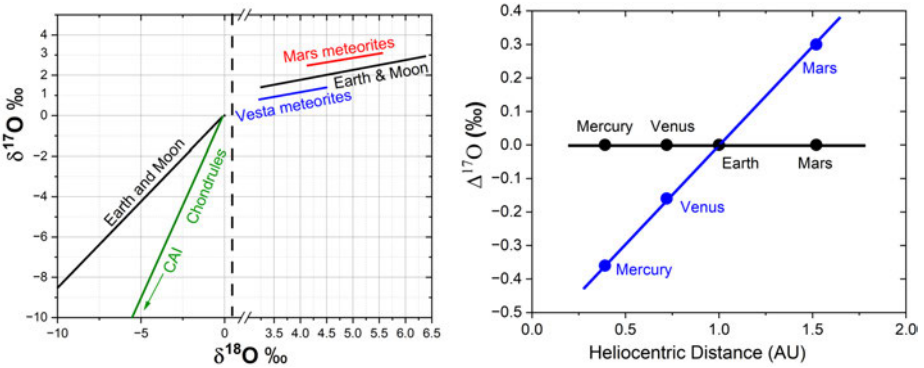

Fig. 2 Left: Schematic showing range of $\delta^{17}O$ and $\delta^{18}O$ planetary values (CAI = Calcium-aluminum inclusions). Lines represent approximate values reported by Scott and Krot (2001) and by Wiechert et al. (2001). On this plot, the Sun would be approximately at −60‰ in both $\delta^{17}O$ and $\delta^{18}O$. Right: Simplified comparison between two mixing scenarios to demonstrate the high precision needed in $\Delta^{17}O$ (‰) measurements that represent the deviation of $d^{17}O$ from the terrestrial fractionation line (TFL) of $\delta^{17}O$ vs. $\delta^{18}O$. Figure 2 above is a simplification of Fig. 15 in Greenwood and Anand (2020) in which the black points and line represent a well-mixed inner solar system, and the blue points and line represent speculation of the expected magnitude of changes in $\Delta^{17}O$ values increasing with heliocentric distance. Distinguishing these two scenarios has important implications for planetary formation and giant impact models, as noted by Greenwood and Anand (2020)

(Theimens and Lin 2021); thus, the triple oxygen (18/17/16) and sulfur (34/33/32) isotopic compositions of various materials have been proposed as probes of early processes in the solar nebula as well as solar system evolution (Theimens 1999). However, to address these questions and discern among processes based on triple-isotope signatures requires much higher precision measurements on extremely low abundance minor isotopes (i.e., ^{17}O and ^{33}S). Figure 2 (left) shows that $\delta^{17}O$ and $\delta^{18}O$ values of the Earth and Moon can be distinguished from those of calcium-aluminum inclusions (CAI) and chondrules at precisions of a few per mil, but meteoritic values are separated by only ~0.5‰. Some models (see example of Fig. 2 right) require even higher precisions in $\delta^{17}O$.

In identifying needed cometary measurements, Mandt et al. (2015) assess that the oxygen and sulfur isotopic measurements are not sufficient to provide any assistance in understanding formation and evolution of the solar system. Although the general trend for cometary $^{16}O/^{18}O$ ratios is consistent with the range described between chondritic material and asteroidal water, more effective classification will require not only more measurements, but also more precise ones that include ^{17}O.

To reveal significant differences in members of the $^{18}O/^{17}O/^{16}O$ triple isotope plots, precisions of ≤1‰ are needed for measurements of $\delta^{17}O$ and $\delta^{18}O$ (Ireland et al. 2020). Likewise, triple isotope precisions in $^{34}S/^{33}S/^{32}S$ require similar or higher precisions in $\delta^{34}S$ and $\delta^{33}S$ for distinguishing meaningful differences among solar system materials (Crockford et al. 2016).

2 Planetary Tunable Laser Spectrometers

Since the development of high-power (mW), single-mode, tunable infrared (1–12 μm) semiconductor lasers that operate at room temperature, tunable laser spectrometer (TLS) instruments have seen widespread application to in situ gas detection (Du et al. 2019; Lackner

2007) and are increasingly considered for planetary payloads (e.g. Table 4 in Miller et al. 2019).

Comprising only a compact laser source and detector coupled to a multi-pass gas cell, single-channel tunable laser spectrometers are simple in concept, design, operation, are easily calibrated, and can be low in volume (0.1–3 liters), mass (0.2–5 kg), and power (1–10 W). With semiconductor lasers of extremely narrow linewidth installed in small packages (1 cm × 1 cm × 0.5 cm), several individual rotation-vibration lines can be scanned over at ultra-high spectral resolution (resolving power $\lambda/\delta\lambda \sim 10$ million). TLS instruments offer high sensitivity (typically $\leq$1 part-per-billion by volume (ppbv)) for a variety of gases identified unambiguously through scanning over more than one line for each species. These compact, low-power instruments are particularly suited to measuring the abundances of low-molecular weight gases (e.g. H_2O, H_2O_2, H_2CO, HOCl, NO, NO_2, HNO_3, N_2O, O_3, CO, CO_2, NH_3, N_2H_4, PH_3, H_2S, SO_2, OCS, HCl, HF, O_2, HCN, CH_4, C_2H_2, C_2H_4, C_2H_6) and to the determination of stable isotope ratios in C, H, N, O and S at high precision (1–2 parts-per-thousand = 1–2‰) (Webster et al. 2013). Early demonstrations of the technique and capability included the first simultaneous measurements of water isotopes HDO, $H_2{}^{16}O$, $H_2{}^{17}O$ and $H_2{}^{18}O$ in Earth's troposphere and stratosphere to reveal dehydration pathways and cirrus origin (Webster and Heymsfield 2003).

Unlike mass spectrometers, tunable laser spectrometers cannot detect noble gases or molecular nitrogen (no change in dipole moment), and do not have gas survey capability. Rather, the laser sources scan over only very narrow (1–2 cm^{-1}) spectral regions that are pre-selected for targeted gases and measurements, the latter validated through HITRAN simulations (Gordon et al. 2017) and laboratory calibrations. The ultra-high spectral resolution of TLS instruments means that even for narrow Doppler-limited lines, the instrument linewidth is negligible, so that the observed lines retain their full absorption depth without broadening, producing high-sensitivity detection. At sampling pressures of ~10 mbar and with modest pathlengths of ~20 m, a TLS instrument has a minimum-detectable mixing ratio of $\leq$1 ppbv for CO, CO_2, OCS, N_2O, HF, NH_3, HCl, NO_2, C_2H_6, CH_4, HCN and PH_3; of 1–3 ppbv for H_2O, C_2H_2, SO_2, HCOOH, O_3, H_2O_2 and HNO_3; and ~5 ppbv for H_2CO, HOCl. H_2S is an unusually weak absorber with a minimum-detection level of ~50 ppbv under these same conditions.

Figure 3 shows the main infrared bands of low-molecular weight gases of interest to planetary science, and an expanded section near 2.63 μm showing water isotope lines, and finally the scan region used by the TLS on SAM-MSL for water isotope ratio measurements.

Planetary tunable laser spectrometers usually employ a closed Herriott cell (Herriott et al. 1964) as the sample cell into which gas is introduced. It has the advantage that moderately long (up to ~20 m) pathlengths can be achieved for the simultaneous use of multiple wavelengths using a single pair of mirrors. In a typical set-up, thermoelectrically-controlled (TEC) infrared semiconductor lasers (diode, interband-cascade (IC), or quantum-cascade (QC)) are used as sources, with their beams bouncing multiple times (typically up to ~100) between two spherical mirror a fixed distance apart (typically 20 cm) (see Fig. 4).

The laser light is injected through a hole (typically ~1 mm in diameter) in the near mirror, and exits usually through a hole in the far mirror, the exiting light falling onto a single-element infrared detector. A 4-channel TLS instrument would have 4 laser source packages, and 4 holes in both the near and far mirrors of the cell, as shown in Fig. 4. For each channel, beam-splitters take a small fraction of the laser light source through a reference cell containing a standard certified gas (i.e. of known isotopic composition) and onto a second set of reference detectors to monitor any spectral line or region motion and to provide on-board calibration data during sampling that may occur years after launch.

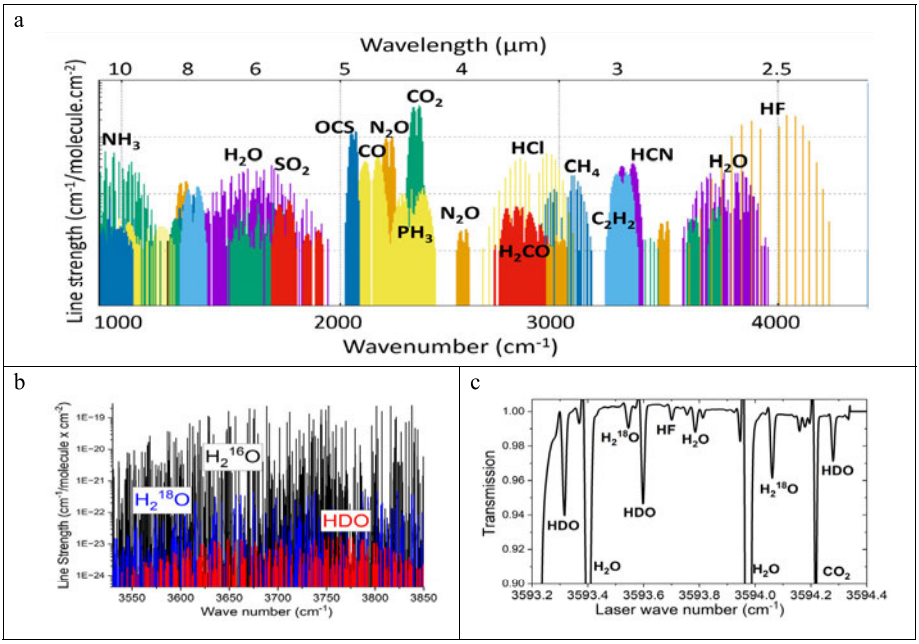

Fig. 3 HITRAN (Gordon et al. 2017) spectral simulations for water. a: HITRAN simulations of major IR absorption bands of various gases from 2.5 to 11 μm, and b: of the numerous water lines near 2.6–2.8 μm. c: actual recorded spectrum from TLS-SAM-MSL (described later in text) during an EGA run (named Avanavero) over a small, carefully-selected region to identify HDO, $H_2{}^{16}O$, and $H_2{}^{18}O$ lines for isotope ratio determinations. Note that this TLS region also identifies HF and CO_2 lines. The optimal spectral region for measuring water isotopes is near 2.63 μm

The sensitivity of tunable laser spectrometers depends on gas pressure, temperature, pathlength and the inherent rotational-vibrational molecular line strength in the chosen wavelength region. Absolute abundance or mixing ratio accuracy is usually limited by systematic errors in the pressure gauge measurement (∼1%) with a smaller contribution from gas temperature error. Because the lasers scan quickly over the spectral region (up to kHz scan rates) and isotope ratios are determined from ratioing the spectral line depth or area of adjacent or nearby lines (e.g. HDO and H_2O, Fig. 3), systematic errors like pressure uncertainty or pathlength uncertainty are to a first order cancelled out, but small temperature errors can in some cases contribute to final isotopic ratio precisions and accuracies.

Classic Herriott cell configurations, even after careful alignment, are limited by the occurrence of optical interference fringes between a variety of reflecting surfaces (Herriott cell mirrors, the laser collimator lens, fore-optics optical elements, and the detector surface itself). These "fringes" have rms amplitudes at best equivalent to a line-depth of $\sim 1 \times 10^{-5}$ (absorption depth of 0.001%) over minutes of integration time (Webster et al. 1994). Several approaches have been used to reduce the amplitude of the optical interference fringes, with varying success (Webster 1985). On the Mars TLS instrument, a very efficient method involved the use of a "fringe-wash" heater on the cell body to cyclically ramp the cell length by a few micrometers during the measurement time (Mahaffy et al. 2012) without reducing spectral resolution. Thermally-driven, tiny changes in mirror separation "move" the phase of fringes in a period shorter than the spectral recording (averaging) time. In this way, the fringes are "washed out" over time, so that the optical fringe amplitude is greatly

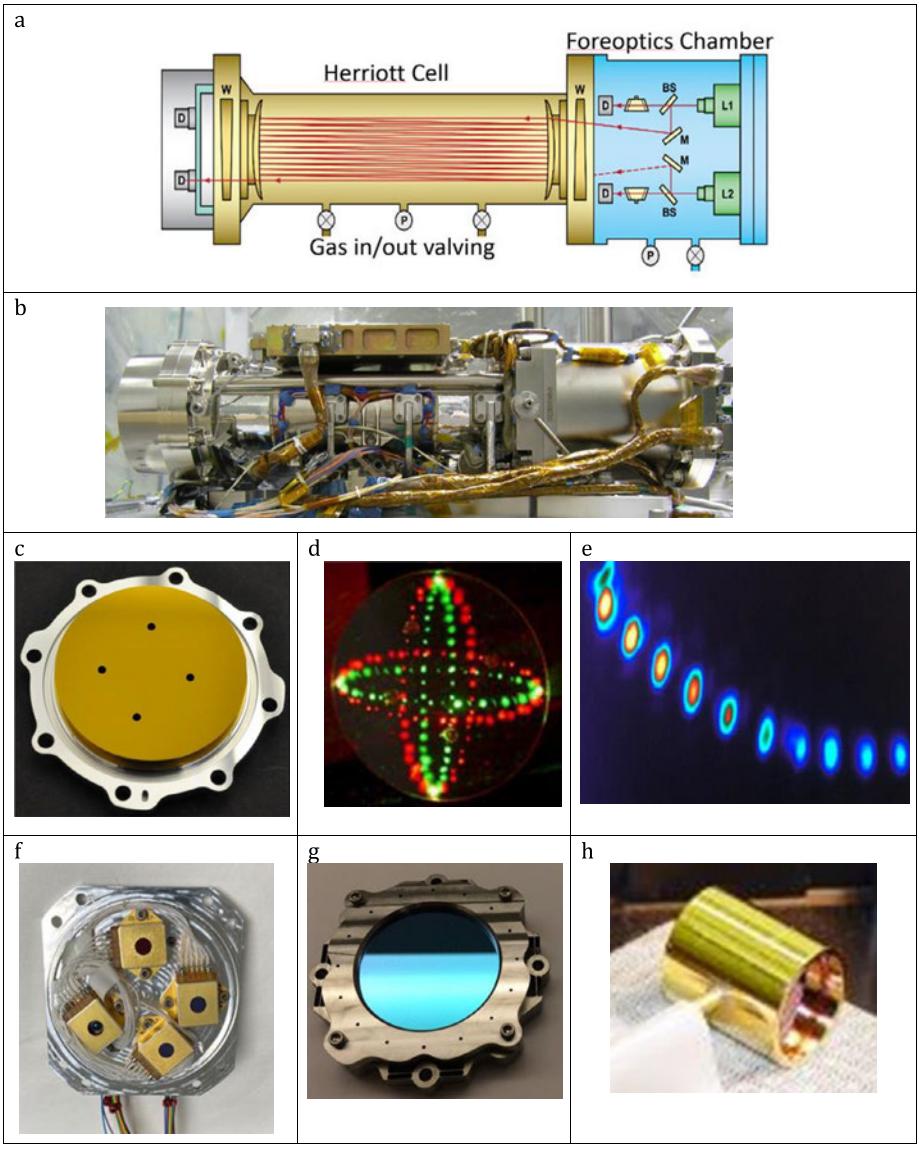

Fig. 4 TLS flight hardware and optical geometry. a: Schematic of the TLS spectrometer showing the laser sources (L), beam-splitters (BS), steering mirrors (M), detectors (D) and wedge windows (W). b: Photo of the 2-channel TLS at delivery to SAM-MSL. c: One of the TLS mirrors showing holes in the aluminum spherical mirror for up to 4-channel injection. d: Visible laser demonstration of the orthogonal spot patterns for the 4-channel option for TLS. e: IR camera image of a section of spots on an IR-transmissive output mirror showing the high beam quality (Webster et al. 2021a). f: Laser packages installed on a prototype new laser plate for 4-channel implementation. g: The wedge window assembly as installed on TLS for MSL, and h: Photo of the 1-cm long reference gas cell(s) used for each channel

reduced through averaging. However, this method requires additional power (up to ∼30 W) for the spectrometer unless the cell normally warms e.g. during an atmospheric probe descent. A newly-invented technique of spot imaging (Webster et al. 2021a) shows promise for significant improvement in sensitivity over traditional methods.

For SAM Evolved Gas Experiment (EGA) runs (Mahaffy et al. 2012), the solid sample is contained in an oven whose temperature is ramped up (typically to over 800 °C) while helium is flowed through the pyrolysis oven. After evacuation of the TLS sample (Herriott) cell to record empty cell values, the TLS cell is opened to receive a "temperature cut" ingest (e.g. 220–330 °C) from the pyrolysis that is introduced into the cell which is subsequently sealed off for analysis. Typically for water, empty cell abundances are extremely low compared to the full cell EGA values so that empty cell subtractions are not needed. Full cell pressures (mainly helium) range from ∼5 to 20 mbar.

The TLS instrument channels (lasers) can be operated individually or simultaneously depending on the mission needs. For all measurements, both empty (evacuated and sealed) and full (sample gas ingested and sealed) cell spectra are recorded for later subtraction should contaminant gas be present in the foreoptics chamber. With the Herriott (sample) cell is filled with gas (typically to 5–20 mbar, pressures at which line broadening does not cause line overlap), a given laser scans over the target spectral region every second, or faster. Onboard, the TLS instrument co-adds these scans to capture average spectra over sequential 1-minute periods that are downloaded. Analysis of each of these 1-minute spectra is done on a line-by-line basis through comparison with HITRAN 2016 calculations (that use terrestrial isotope standard delta values), so that volume mixing ratios are retrieved for each of the target lines (e.g. for H_2O, HDO and $H_2{}^{18}O$). Average values of the volume mixing ratios for H_2O, HDO and $H_2{}^{18}O$ are then calculated from each of the 1-minute spectra. During the run, typically 10–30 full-cell spectra are recorded, so that the 10–30 values retrieved of average abundance values can be ratioed and statistically analyzed to find the mean value with standard errors of either 67% confidence interval (CI) or 95% CI. In our example here, ratioing the HDO and $H_2{}^{18}O$ mean abundance with that determined for H_2O provides the δD and $\delta^{18}O$ values and their propagated errors.

Planetary TLS instruments have high flexibility in data rates and data volume that can be tailored to the specific mission. In general, each channel/laser produces direct absorption and second harmonic (2f) spectra for both the Herriott cell path and for the reference gas cell, i.e. each channel produces 4 spectra in addition to housekeeping data (e.g. cell temperatures, pressures etc.). As an example, with 1024 spectral points in a single spectrum and a measurement frequency of 15 seconds for each data point, in a 10-minute data collection, a 2-channel TLS would produce ∼5 Mbits of total data at an average rate of ∼50 kbits/sec.

3 Advantages of Coupling Planetary Tunable Laser Spectrometers with Mass Spectrometers

Like planetary mass spectrometers, tunable laser spectrometers offer wide flexibility in making in situ measurements of both planetary atmospheres and of gases evolved from heating surface samples. To build upon the pioneering early measurements of isotope ratios in solar system bodies, in some cases higher precisions are required to discriminate various potential processes and provide input for models of formation and evolution. As discussed in Sect. 1, precisions of ∼20–50‰ are needed in measurements of δD and $\delta^{15}N$. For $\delta^{13}C$ and $\delta^{18}O$, precisions of ∼10‰ or better are needed. For interpretations of triple isotope data in both O and S, precisions of 2–5‰ or better are needed.

Tunable laser spectrometer (TLS) instruments offer several unique capabilities for in situ planetary exploration that complement and expand the measurement capabilities of mass spectrometers. The TLS has unique capability in the lower mass region to disentangle contributions from methane, water and ammonia in particular, and to allow precise determination of isotope ratios in these simple gases without ambiguity from mass interferences. TLS spectrometers offer:

1. High-sensitivity detection (∼1 ppbv) of a wide variety of gases present in planetary atmospheres or evolved from heating of planetary surface materials (rocks, ices), including H_2O, H_2O_2, H_2CO, HOCl, NO, NO_2, HNO_3, N_2O, O_3, CO, CO_2, NH_3, N_2H_4, PH_3, H_2S, SO_2, OCS, HCl, HF, O_2, HCN, and CH_4, C_2H_2, C_2H_4, C_2H_6.
2. Detection of trace or disequilibrium species (e.g. CH_4, H_2S, NH_3, PH_3) and better determination of isotope ratios in low-abundance gases. With typically 1000 times the detection sensitivity of planetary mass spectrometers in regions of isobaric interferences, TLS instruments can readily distinguish CO from N_2.
3. High-precision isotope ratio measurements in molecules containing C, H, N, O, S over a large dynamic range. Precisions of ∼1–2‰ are typically ∼10 times better than a planetary mass spectrometer. With spectra recorded every fraction of a second, the measurements are simultaneous for any given gas sample.
4. The unique ability to measure the triple isotope ratios in O and S, for example $^{18}O/^{17}O/^{16}O$ in CO_2 and H_2O, and $^{34}S/^{33}S/^{32}S$ in SO_2 and OCS.

4 The First Planetary TLS Instruments

A tunable diode laser spectrometer was first considered for a planetary mission as part of the Cassini Huygens probe (Webster et al. 1990) during the European Space Agency (ESA) Phase A study. It was an open-path multi-channel instrument to measure abundances of CO and isotopologues at 4.7 μm, HCN and C_2H_2 at 3.0 μm, C_2H_6, CH_4 and isotopologues at 3.4 μm, and possibly C_2N_2. The doughnut-shaped Herriott cell mirrors (see Fig. 5a) allowed the inclusion of a visible-laser-based particle size spectrometer along the central axis. However, laser source technology was immature, since the lasers had to be cooled to 80 K with a Joule-Thomson cooler whose high-pressure reservoir was considered a mission risk, so the instrument was not carried forward into Phase B.

Two versions of TLS (May et al. 2001), an open-path meteorological sensor (see Fig. 5b) and a closed-cell EGA analyzer, both tailored for water at 1.37 μm and carbon dioxide at 2 μm, were flown on the Mars98 Mars Volatile and Climate Surveyor (MVACS) payload (PI David Paige, UCLA) on the Mars Polar Lander (MPL). After successful atmospheric entry, MPL crashed (Dec. 1999) on the Martian surface at high velocity after premature termination of the engine firing. Associated with the same mission, two identical probes, named the New Millennium Deep-Space 2 (DS2) probes carried a circuit-board-mounted tunable diode laser operating at 1.37 μm with a short pathlength (∼2 cm) (see Fig. 5c) with a goal to penetrate the surface of Mars and measure the evolved water abundance. DS2 was designed to detach from MPL and fall to the surface using an aeroshell impactor, but with no parachute. The mission was declared a failure in March 2000 after communication with the probe could not be established.

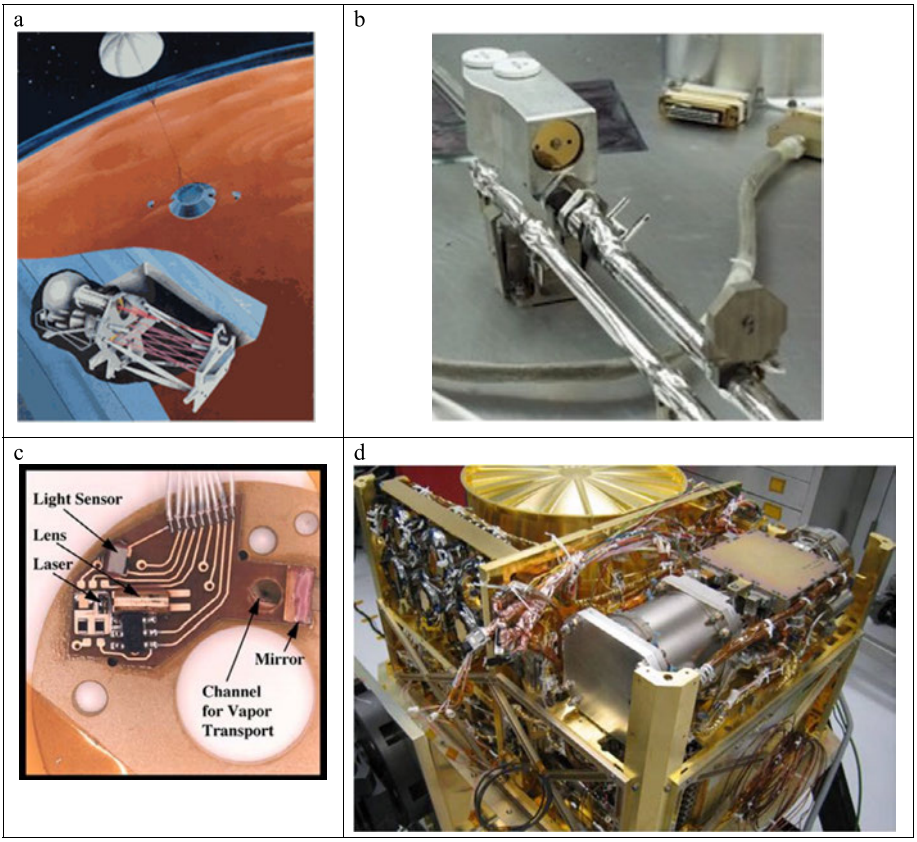

Fig. 5 a: Artist concept of the Huygen's Probe TLS (not flown; Webster et al. 1990). b: Photograph of the MVACS open-path, mast-mounted TLS (May et al. 2001) for CO_2 and H_2O. c: Final layout of the circuit-board-mounted TLS on the DS-2 probe. d: Photograph of TLS (foreground) being installed into the SAM instrument suite for the Mars Curiosity rover

5 Performance at Mars on the Curiosity Rover

The two-channel Tunable Laser Spectrometer (TLS) operating within the Sample Analysis at Mars (SAM) instrument suite on the Mars Science Laboratory (MSL) Curiosity rover (Mahaffy et al. 2012) is configured as shown in Fig. 4, with a tunable diode laser source at 2.78 μm for water and carbon dioxide, and an interband cascade source at 3.27 μm for methane measurements. The SAM suite includes a Quadrupole Mass Spectrometer (QMS), and a Gas Chromatograph (GC). A sample handling and processing system includes enrichment capability for noble gases and for methane, and a pyrolysis oven in which solid samples are heated in a helium flow to allow Evolved Gas Analysis (EGA) or combustion experiments.

Operating successfully on the Mars Curiosity rover for over 10 years, all 3 SAM instruments have individually produced first-of-a-kind measurements on both the Martian atmosphere and on gases evolved from rock pyrolysis (Vasavada 2022). For TLS, this includes determination of CO_2 $^{13}C/^{12}C$ and $^{18}O/^{17}O/^{16}O$ isotope ratios, as well as D/H and $^{18}O/^{16}O$

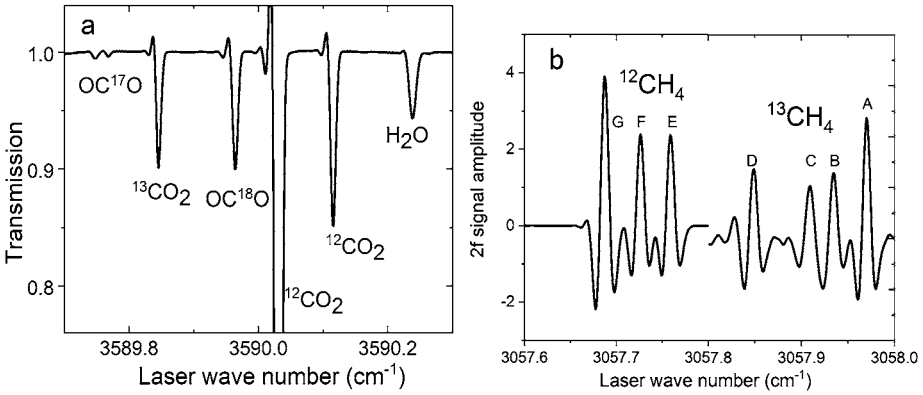

Fig. 6 Actual recorded spectra from TLS a: A single 30-second TLS spectrum of the region near 2.78 μm. This spectrum is one of 60 such sequential spectra recorded for a single run on Mars sol 2897 (since landing) to measure $^{13}C/^{12}C$ and $^{18}O/^{17}O/^{16}O$ in Mars atmospheric CO_2 on that day. This same scan region is used in EGA experiments. By offsetting the laser temperature stabilization, this same laser channel is also able to switch to the water isotope region shown earlier in Fig. 3. b: actual methane spectra recorded in a SAM EGA run for the Cumberland-3 sample pyrolysis, showing the 3 parent $^{12}CH_4$ lines and the 4 $^{13}CH_4$ lines used to determine the $^{13}C/^{12}C$ ratio in methane. The $^{13}CH_4$ line region has been expanded in the vertical axis by a factor of ~50. This panel b is an adaptation of that presented in House et al. (2022)

in water using the 2.78 μm channel, and the detection of atmospheric CH_4 and its $^{13}C/^{12}C$ isotope ratio in EGA experiments using the 3.27 μm channel.

In the Martian atmosphere, TLS-SAM reported delta values of $\delta^{13}C_{PDB} = 46 \pm 2‰$ and $\delta^{18}O_{VSMOW} = 48 \pm 2‰$ (updated from Webster et al. 2013) in CO_2 that reveal the extent of atmospheric escape processes that leave behind an atmosphere enriched in is C, H, N and O content. Additionally, in atmospheric CO_2 TLS measured $\delta^{17}O$ and the clumped isotope $\delta^{13}C$ $\delta^{18}O$ at lower precisions (Webster et al. 2013).

In EGA and stepped combustion experiments, measurements of the $^{13}C/^{12}C$ in CO_2 showed variability in $\delta^{13}C_{PDB}$ from ~−20‰ to ~+40‰ (Leshin et al. 2013; Stern et al. 2022). In methane, carbon isotopic values ($\delta^{13}C$) of the methane released during pyrolysis of 24 powder samples showed a high degree of variation (~−140 to ~+20‰) that included ten measurements of $\delta^{13}C_{PDB}$ values less than −70‰ in six different sampling locations. Multiple plausible explanations were described for the anomalously-depleted ^{13}C (House et al. 2022).

Measurements of D/H and $^{18}O/^{16}O$ in water have been made over numerous pyrolysis EGA runs to reveal a relatively tight range in $\delta^{18}O$ (20–80‰) and an expected wider range to the measured δD values (2000–4500‰). Variation is seen along the rover traverse through a stratigraphic sequence of a diverse array of sedimentary facies interpreted (Hofmann et al. 2023) to reflect formation in fluvial, deltaic, lacustrine, and eolian environments, sampling rocks from each setting along the way. These measurements represent the first time simultaneous paired isotopes in water have been measured in situ on any planet outside Earth. In a stepped combustion experiment at various temperatures of a ~3 billion-year-old Hesperian clay mudstone, nearly identical enriched D/H ratios of ~3 times Standard Mean Ocean (SMOW) were measured in both H_2O (TLS) and in H_2 (QMS). This value revealed crucial information regarding the history of water loss on Mars (Mahaffy et al. 2015), showing that when the clay formed, Mars had already lost about half of its water, having a global equivalent layer of water of ~150 m.

By taking advantage of the sophisticated gas processing system of SAM that allows atmospheric methane to be effectively enriched by a factor of 25 by use of a CO_2 scrubber, TLS was able to record the low (~0.4 ppbv) background levels of methane seen at night in the near-surface atmosphere. A repeatable seasonal variation between northern spring and northern summer was observed over the 10-year period of MSL operations. Importantly, a day-night-day sequence showed that TLS detected no methane during the daytime (Webster et al. 2021b), consistent with the absence of methane reported by the ExoMars Trace Gas Observer instruments (Korablev et al. 2019).

6 Mars Instrument Concepts

TLS instruments using either closed-cell or open-path geometries have been considered for a variety of platforms on Mars, including balloons, aerobots, airplanes, rovers, landers, probes, and ice drill ice components.

Under NASA's Mars Scout opportunities of the late 1990's and early 2000's, TLS instruments were included in proposals for multiple met stations (Webster et al. 2004; PI Haberle, NASA Ames), for multiple miniature lander stations (PI Paige, UCLA), on a Mars balloon (PI Mahaffy, NASA GSFC) that paired a MS and TLS for the first time, carrying a telescope to receive light from a multi-channel TLS sensing a variety of gases including methane, and on two Mars airplane proposals (ARES, PI Levine; PI Calvin). In the airplane versions, the TLS would have directed its milliwatt-level laser sources down to the Martian surface, and used a 15-cm diameter telescope to return the topographically-scattered return light, thereby achieving long folded pathlengths of ~a few kilometers for ultrahigh sensitivity, detecting gases to a few parts-per-trillion.

One Mars Scout proposal named CHRONOS (PI Hecht, JPL) focused on the isotopic analysis of water vapor released from heated Martian ice cores during a descending drill. The payload included miniature instruments (TLS, microscopic camera) travelling down a borehole of several centimeters in diameter to record layering and the density of dust particle layers intertwined within the ice deposition records. The stratigraphic profile would have included temperature, dust density, oxygen isotope fractionation, pH, conductivity, and redox potential. A more recent proposal included an open-path micro-TLS as part of the payload of a "Mars Drop" (PI Staehle, JPL) to study geographic/temporal variations in the episodic release of methane in Mars' atmosphere and potential correlations with changes in water vapor.

7 VTLS for Venus Atmospheric Probe

The Venus Tunable Laser Spectrometer (VTLS) is part of the recently-selected NASA mission named Deep Atmosphere Venus Investigation of Noble Gases, Chemistry and Imaging (DAVINCI, Garvin et al. 2022). DAVINCI consists of an orbiter that records flyby data before sending a descent probe into the Venus atmosphere. Current launch year is 2029. In addition to VTLS (lead Webster), the probe payload includes a Venus Mass Spectrometer (VMS, lead Malespin), a UV and NIR imaging (VISOR, lead Ravine), an atmospheric structure instrument (VASI, lead Lorenz), and a Venus Descent Imager (VENDI, lead Ravine).

During the ~1-hour descent, VMS will measure noble gas abundances and their isotope ratios and conduct survey measurements (see Fig. 7). Both VMS and VTLS will record the vertical mixing ratio profiles of several gases including H_2O, CO, CO_2, OCS, SO_2, and H_2S.

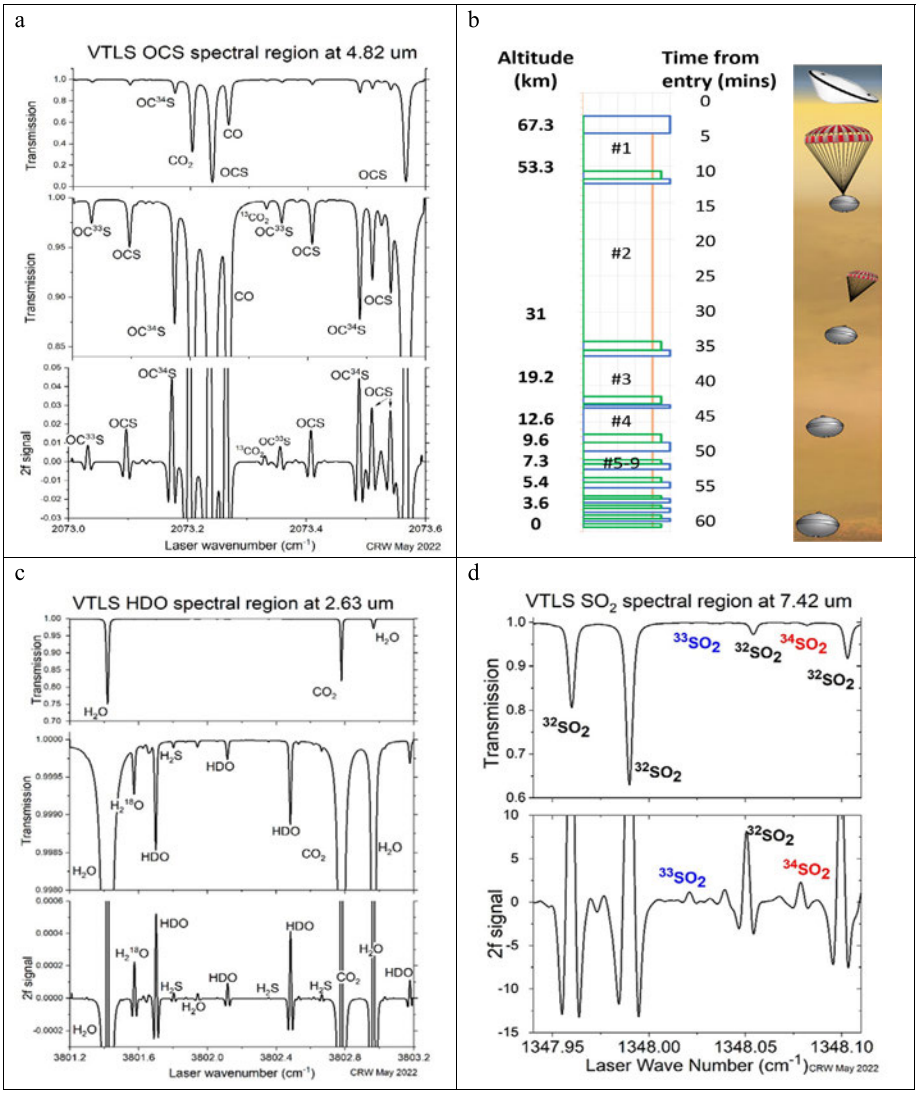

Fig. 7 VTLS scan regions (a, c and d), and planned sample timing sequence (b). The spectra are HITRAN simulations (Gordon et al. 2017) using a cell pressure of 20 mbar, a pathlength of 1620 cm, temperature of 318 K, and volume mixing ratios of 30 ppmv for OCS and H_2O, 3 ppmv for H_2S, and 150 ppmv for SO_2 in a mainly CO_2 atmosphere. The upper panel(s) are the direct absorption spectra while the lowest panels are the zero-based second-harmonic spectra. Panel b shows the nominal timing sequence for VTLS cell gas ingest (blue), pump (green) and closed-cell integration time (orange) with the central numbers referring to the nominal sample number. A graphic representing the descent probe sequence is also shown in panel b

VTLS will focus on high-precision (~2‰) isotope ratio measurements of D/H and $^{18}O/^{16}O$ in water, of $^{13}C/^{12}C$ in CO_2, and the triple isotope ratios $^{34}S/^{33}S/^{32}S$ in both SO_2 and OCS.

VTLS is a 3-channel spectrometer based largely on the heritage of the TLS-SAM-MSL Instrument, with target measurements of:

Channel 1 at 2.63 μm: H_2O, H_2S; D/H and $^{18}O/^{16}O$ in H_2O
Channel 2 at 4.82 μm: CO, OCS, CO_2, $^{34}S/^{33}S/^{32}S$ in OCS, $^{13}C/^{12}C$ in CO_2
Channel 3 at 7.4 μm: SO_2 and $^{34}S/^{33}S/^{32}S$ in SO_2.

In the MSL version, the SAM suite (Mahaffy et al. 2012) provided cell evacuation of TLS using its wide-range turbomolecular pumps, and cell filling through atmospheric ingest or helium flow in EGA experiments. For DAVINCI, VTLS will receive atmospheric samples through inlets and flow restrictors tailored to maintain a Herriott cell pressure close to 30 mbar for optimal detection. To cover the rapidly-increasing Venus pressure during descent, 4 different flow restrictors are needed.

VTLS cell evacuation is achieved using molecular sieve (Linde 13X) pumping with a dedicated pumping volume, and a second volume used to maintain flow to minimize memory affects during the one-hour descent. VTLS has a cell pump/sample ingest sequence that provides ∼10 specific samples to be ingested with integration times ranging from 20 minutes in the upper atmosphere to 30 seconds in the lower atmosphere samples. The integration time period results from the need to focus on water in the upper atmosphere, while the short integration times of the lower atmosphere are to sequence a higher cadence prior to landing. VTLS uses an interband-cascade laser for channel 1 at 4.82 μm, a tunable diode laser for channel 2 at 2.63 μm, and a quantum-cascade laser for channel 3 at 7.42 μm. Heat generated by the simultaneously-operating three lasers is dissipated from the laser plate directly into a thermal storage unit (TSU) attached to the laser plate. The TSU contains a paraffin wax phase-change material that efficiently absorbs heat during its transition temperature of 19 °C.

8 TLS on an Icy Body Lander

In combination with a mass spectrometer, TLS has been proposed as part of the payload of a Discovery program lander to Ceres (mission PI House, Penn State), and is considered in the in-situ science options for several Enceladus surface mission concepts (Combes et al. 2008; Sekine et al. 2014; Mousis et al. 2022) including a New Frontiers lander (PI House, Penn State). In these missions, the heating and volatilization of icy surface material provides relatively large amounts of the evolved gases for the instruments. For TLS, in addition to stable isotope ratios in C and O, of great interest would be to determine the H_2O/NH_3 ice ratios, the $^{15}N/^{14}N$ isotope ratio in ammonia and the D/H in both species. Figure 8 shows one example spectral region that an Enceladus TLS might access to determine the isotope ratios in ammonia evolved from heating surface ice.

9 TLS Capability on a Saturn Probe

Giant planets offer the best opportunity to reveal the conditions of the primordial solar nebula from which all solar system bodies formed (Atreya et al. 2020), in part because loss of volatiles (even hydrogen) is insignificant since their formation ∼4.6 billion years ago. For planetary probes that can reach down to ∼10 bars, the gas giants (Jupiter and Saturn) offer easier access to planetary data than do the Ice Giants Uranus and Neptune.

A Saturn atmospheric probe was proposed under NASA's New Frontiers 4 program (Banfield et al. 2018, Mission PI Amy Simon, NASA GSFC) and will be proposed again in future opportunities. In addition to other instruments, a Saturn probe would carry both a mass spectrometer and a tunable laser spectrometer. As part of a descending probe payload, a TLS instrument would work in concert with a mass spectrometer to focus on low molecular

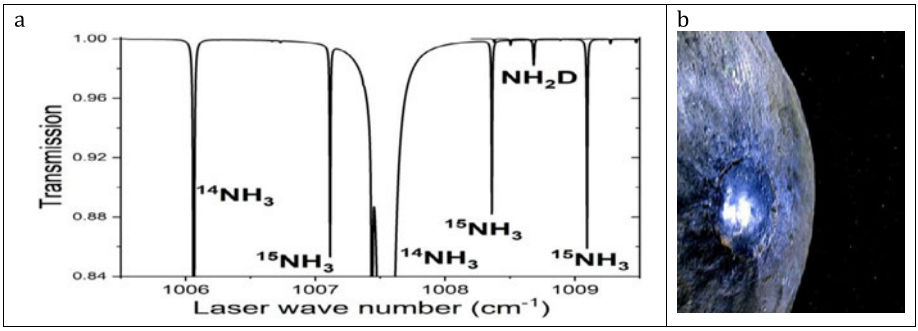

Fig. 8 a: Calculated spectrum near 9.92 μm of ammonia and its isotopic forms showing line positions and relative depths using terrestrial isotope ratios. In this region with well-isolate lines, TLS could determine $^{15}N/^{14}N$ and D/H simultaneously in evolved gas samples to augment measurements in a second channel of water isotopes. The spectral scan is generated using line parameters of HITRAN for $^{15}NH_3$ and $^{14}NH_3$, and for NH_2D developed by K. Sung at JPL (personal communication) modified by line intensities from Job et al. (1987). This plot represents what might be seen in an EGA spectrum for a NH_3 mixing ratio of 0.2% in which the strong $^{14}NH_3$ line near 1006 cm^{-1} is ∼48% deep. The existence of the very strong $^{14}NH_3$ line at 1007.5 cm^{-1} would allow very large dynamic range in determining the NH_3 abundance. b: Photo of Ceres, courtesy NASA

weight gases expected in low abundances, and in high-precision isotope ratios in C, H, N, and O, as tabulated in Table 1.

10 TLS Capability at the Ice Giants Uranus and Neptune

In situ exploration of the Ice Giants Uranus and Neptune is more constrained than that of the Gas Giants, whose temperatures are much warmer compared to the Ice Giants at comparable depth pressure limits of ∼10 bar. Thus CH4 remains gaseous on Jupiter and Saturn, allowing a determination of the carbon elemental ratio from bulk CH4 abundance. The well mixed region of H2S was reached at around 15 bars on Jupiter, which allowed the determination of the sulfur elemental ratio from the Galileo probe (Niemann et al. 1998; Atreya et al. 1999; Wong et al. 2004). The well-mixed region of the other condensible species, NH3 and H2O, on Jupiter is much deeper, however, perhaps tens of bars or even greater than 100 bars, as Juno found (Li et al. 2017, 2021). In contrast to the Gas Giants, because of the much colder temperatures of the Ice Giants, even CH4 condenses and the well-mixed region of the other condensibles, NH3, H2S and H2O, is expected to be much deeper than in the atmospheres of the Gas Giants, which would prevent the determination of the C, N, S and O elemental abundance on an entry probe designed for 10 bars (Atreya et al. 2020). Noble gases will be well-mixed for all giant planets and remain critical measurements to be made. As emphasized in the introduction, the focus needs to be on precision isotope measurements and gradients in density profiles of CH_4, NH_3, H_2S and H_2O, rather than their bulk abundance. To that end, with gas sensitivities ∼1000 times higher than that current probe-accommodatable flight mass spectrometers, a TLS instrument has the best opportunity for making these measurements.

To assess TLS capability at Uranus (see Table 2), we assume that at probe depths of ∼10 bars, expected mixing ratios would be ∼5% for CH_4, ∼1 ppmv for NH_3, ∼20 ppmv for H_2S, and only 1–2 ppbv for H_2O (Atreya et al. 2020 nominal model). A TLS with a typical limit

Table 1 Calculated TLS capabilities for a giant planet probe

TLS channel	Wavelength (μm)	Molecules	Expected mixing ratio	Detection limit for MSL configuration with 81 passes	STLS capability	Abundance accuracy and isotope ratio precision
1	2.64	H_2O, HDO, $H_2{}^{17}O$, $H_2{}^{18}O$	700 ppmv	1 ppmv	H_2O abundance	2%
					D/H in water	0.5%
					$^{18}O/^{17}O/^{16}O$ in water	0.5%
		H_2S	77 ppmv	300 ppbv	H_2S abundance (no isotopes)	2%
2	3.27	CH_4, $^{13}CH_4$, CH_3D	5000 ppmv	1 ppbv	CH_4 abundance	2%
					$^{13}C/^{12}C$ in methane	0.2%
					D/H in methane	0.5%
		C_2H_6	5 ppmv	0.3 ppbv	C_2H_6 abundance (no isotopes)	2%
3	4.18	PH_3, PH_2D	2–5 ppmv	1 ppbv	PH_3 abundance	2%
					D/H in phosphine	0.5%
4	9.92	NH_3, $^{15}NH_3$, NH_2D	200–1000 ppmv	1 ppbv	NH_3 abundance	2%
					$^{15}N/^{14}N$ in ammonia	0.2%
					D/H in ammonia	0.5%
Other possibilities:						
	4.6	CO	1 ppbv	0.2 ppbv	CO abundance (no isotopes)	20%
	3.0	HCN, C_2H_2	TBD	0.8 ppbv	-HCN and C_2H_2 abundances	2%
	2.55	HF	TBD	0.2 ppbv	HF abundance	2%
	2.59	$H_2{}^{32}S$, $H_2{}^{33}S$, $H_2{}^{34}S$	77 ppmv	150 ppbv	H_2S abundance	2%
					- triple S isotopes, ^{32}S, ^{33}S and ^{34}S of limited precision	0.5%

Table 2 Expected mixing ratios at Uranus and TLS capabilities

Gas	Expected vmr	TLS abundances	TLS isotope ratios
CH_4	5%	CH_4 abundance at 2% uncertainty, LOD is 1 ppbv	$^{13}C/^{12}C$ in CH_4 to 2‰
			D/H in CH_4 to 10‰
NH_3	1 ppmv	NH_3 abundance at 2% uncertainty, LOD is 0.2 ppbv at 10.7 μm	$^{15}N/^{14}N$ to 50‰
H_2O	1–2 ppbv	H_2O LOD is 1 ppbv	Not possible
H_2S	20 ppmv	H_2S abundance at 2% uncertainty, LOD is 50 ppbv	$^{34}S/^{32}S$ to 10%

of detection at ∼1 ppbv could readily determine condensible mixing ratios and gradients of CH_4, NH_3 and H_2S, but would struggle to detect H_2O at its very low mixing ratio. For a water abundance of only 1 ppbv, HDO and $H_2{}^{18}O$ spectral line absorptions would be too weak to detect, so that isotope ratios in D/H and $^{18}O/^{16}O$ would not be possible even if

enriched to greater than twice the solar value (Cavalie et al. 2020 and references therein). HITRAN simulations show that for NH_3, the $^{15}NH_3$ lines in the region of Fig. 8 would have a combined depth of $\sim 20 \times 10^{-5}$, providing a SNR of ~20. Therefore, the $^{15}N/^{14}N$ ratio could be determined to ~50‰ and the D/H in NH_3 to ~30% at best. Hydrogen sulfide H_2S is an unusually weak infrared absorber, so that at 2.7 μm wavelength, while abundances could be retrieved down to a limit-of-detection (LOD) of ~50 ppbv, isotope ratios in $^{34}S/^{32}S$ could only be determined to ~10%. Methane is readily detected by a TLS instrument (Webster et al. 2021b) and at a Uranus mixing ratio of 5%, the $^{13}C/^{12}C$ ratio could be determined to ~2‰ and the D/H in CH_4 to ~10‰.

With the high mixing ratios expected for CH_4 and NH_3, a micro-TLS instrument (e.g. as demonstrated as a methane-sniffer for Pacific Gas and Electric Company by Lance Christensen at JPL) with short pathlengths of only 1–20 cm could be employed on multiple atmospheric probes at Uranus (Wong et al. 2024).

In conclusion, as already demonstrated on Mars, and in preparation for Venus, the combination of a mass spectrometer and a tunable laser spectrometer provides the best possible instrumentation in a small package for in situ gas abundances and isotopic ratios measured either in planetary atmospheres or in gases evolved from vaporizing surface samples.

Acknowledgements This research was carried out in part at the Jet Propulsion Laboratory, California Institute of Technology, under a contract with the National Aeronautics and Space Administration (80NM0018D0004). ©2023. California Institute of Technology. Government sponsorship is acknowledged. The authors recognize the significant contribution to developing the JPL tunable laser spectrometers by engineering staff at JPL (including Greg Flesch, Didier Keymeulen, Ryan Briggs, David Cohen) and at NASA GSFC (including Charles Malespin, Micah Johnson and Oren Sheinmann).

Declarations

Competing Interests The authors have no relevant financial or non-financial interests to disclose, and no competing interests to declare that are relevant to the content of this article.

References

Arevalo R Jr, Ni Z, Danell RM (2019) Mass spectrometry and planetary exploration: a brief review and future projection. J Mass Spectrom 55(1):e4454. https://doi.org/10.1002/jms.4454

Arevalo R et al (2023) Laser desorption mass spectrometry with an Orbitrap analyser for in situ astrobiology. Nat Astron 7:359–365

Atreya SK, Wong MH, Owen TC, Mahaffy PR, Niemann HB, de Pater I, Drossart P, Encrenaz T (1999) A comparison of the atmospheres of Jupiter and Saturn: deep atmospheric composition, cloud structure, vertical mixing, and origin. Planet Space Sci 47:1243–1262

Atreya SK, Hofstadter MH, In JH, Mousis O, Reh K, Wong MH (2020) Deep atmosphere composition, structure, origin, and exploration, with particular focus on critical in situ science at the icy giants. Space Sci Rev 216(1):18. https://doi.org/10.1007/s11214-020-0640-8

Balsiger H et al (2007) Rosina – Rosetta orbiter spectrometer for ion and neutral analysis. Space Sci Rev 128:745–801

Banfield D et al (2018) SPRITE: a Saturn probe New Frontiers mission. In: IEEE aerospace conference proceedings, Big Sky Montana. https://doi.org/10.1109/AERO.2018.8396829
Barnes JW et al (2021) Science goals and objectives for the dragonfly titan rotorcraft relocatable lander. Planet Sci J 2:130
Bolton SJ et al (2017) Jupiter's interior and deep atmosphere: the initial pole-to-pole passes with the Juno spacecraft. Science 356:821–825. https://doi.org/10.1126/science.aal2108
Brockwell TG, Meech KJ, Pickens K et al (2016) The mass spectrometer for planetary exploration (MASPEX). In: 2016 IEEE aerospace conference
Cavalie T et al (2020) The deep composition of Uranus and Neptune from in situ exploration and thermochemical modeling. Space Sci Rev 216:58. https://doi.org/10.1007/s11214-020-00677-8
Chou L et al (2021) Planetary mass spectrometry for agnostic life detection in the solar system. Front Astron Space Sci 8:173
Combes M, de Bergh C, Luz D, Sicardy B (2008). TANDEM (Titan and Enceladus Mission) workshop, 17–19 March 2008, Chateau de Meudon, 92195 Meudon, France
Crockford PW et al (2016) Triple oxygen and multiple sulfur isotope constraints on the evolution of the post-Marinoan sulfur cycle. Earth Planet Sci Lett 435:74–83
de Pater I, Romani PN, Atreya SK (1989) Uranus' deep atmosphere revealed. Icarus 82:288–313. https://doi.org/10.1016/0019-1035(89)90040-7
de Pater I, Romani PN, Atreya SK (1991) Possible microwave absorption by H2S gas in Uranus' and Neptune's atmospheres. Icarus 91:220–233. https://doi.org/10.1016/0019-1035(91)90020-T1
Deligny C, Füri E, Deloule E, Peslier AH, Faure F, Marrocchi Y (2023) Origin of nitrogen on Mars: first in situ N isotope analyses of martian meteorites. Geochim Cosmochim Acta 344:134–145. https://doi.org/10.1016/j.gca.2023.01.017
Dones L et al (2015) Origin and evolution of the cometary reservoirs. Space Sci Rev 1–4:191–269
Du Z, Zhang S, Li J, Gao N, Tong K (2019) Mid-infrared tunable laser-based broadband fingerprint absorption spectroscopy for trace gas sensing: a review. Appl Sci 9:338. https://doi.org/10.3390/app9020338
Feuchtgruber H et al (2013) The D/H ratio in the atmospheres of Uranus and Neptune from Herschel PACS observations. Astron Astrophys 551:A126. https://doi.org/10.1051/0004-6361/201220857
Garvin JB et al (2022) Revealing the mysteries of Venus: the DAVINCI mission. Planet Sci J 3(5):117. https://doi.org/10.3847/PSJ/ac63c2
Goetz W et al (2016) MOMA: the challenge to search for organics and biosignatures on Mars. Int J Astrobiol 15:239–250
Gordon IE et al (2017) J Quant Spectrosc Radiat Transf 203:3–69 https://doi.org/10.1016/j.jqsrt.2017.06.038
Greenwood RC, Anand M (2020) What is the oxygen isotope composition of Venus? The scientific case for sample return from Earth's "sister" planet. Space Sci Rev 216:52
Herriott DR, Kogelnik H, Kompsner R (1964) A scanning spherical mirror interferometer for spectral analysis of laser radiation. Appl Opt 3:1471–1484
Hoffman JH, von Oyama VI, Zahn U (1980) Measurement of the Venus lower atmosphere composition – a comparison of results. J Geophys Res 85:7871–7881
Hofmann A et al (2023). Water isotope paper. In preparation
Hörst SM (2017) Titan's atmosphere and climate. J Geophys Res. https://doi.org/10.1002/2016JE005240
House CH et al (2022) Depleted carbon isotope compositions observed at Gale crater, Mars. Proc Natl Acad Sci 119(4):e2115651119
Ireland TR, Avila J, Greenwood RC, Hicks LJ, Bridges JC (2020) Oxygen isotopes and sampling of the solar system. Space Sci Rev 216:25
Irwin PGJ, de Bergh C Courtin R et al (2012) Icarus 220:369–382
Jakosky BM, Slipski M, Benna M, Mahaffy P, Elrod M, Yelle R, Stone S, Alsaeed N (2017) Mars' atmospheric history derived from upper-atmosphere measurements of Ar-38/Ar-36. Science 355:1408–1410
Job VA, Kartha SB, Singh K, Kartha VB (1987) J Mol Spectrosc 126:290
Kasprzak WT, Niemann HB, Hedin AE, Bougher SW, Hunten DM (1993) Neutral composition measurements by the Pioneer Venus Neutral Mass-Spectrometer during Orbiter reentry. Geophys Res Lett 20:2747–2750
Kasprzak WT et al (2007) Cassini Orbiter Ion and Neutral Gas Mass Spectrometer (INMS) results. In: Workshop on Planetary Atmospheres, held November 6–7, 2007 in Greenbelt, Maryland. LPI Contribution No. 1376, p 59
Korablev O et al (2019) No detection of methane on Mars from early ExoMars Trace Gas Orbiter observations. Nature 568:517–520
Lackner M (2007) Tunable diode laser spectroscopy in the process industries: a review. Rev Chem Eng 23(2):65. https://doi.org/10.1515/REVCE.2007.23.2.65
Leshin L et al (2013) Volatile, isotope, and organic analysis of Martian fines with the Mars Curiosity rover. Science 341:1238937. https://doi.org/10.1126/science

Li C et al (2017) The distribution of ammonia on Jupiter from a preliminary inversion of Juno microwave radiometer data. Geophys Res Lett 44:5317–5325
Li C et al (2020) The water abundance in Jupiter's equatorial zone. Nat Astron 4(6):609–616. https://doi.org/10.1038/s41550-020-1009-3
Mahaffy PR, Niemann HB, Alpert A, Atreya SK, Demick J, Donahue TM, Harpold DN, Owen TC (2000) Noble gas abundances and isotope ratios in the atmosphere of Jupiter from the Galileo probe mass spectrometer. J Geophys Res 105(E6):15061–15071. https://doi.org/10.1029/1999JE001224
Mahaffy PR et al (2012) The sample analysis at Mars investigation and instrument suite. Space Sci Rev 170:401–478
Mahaffy PR et al (2014) The Neutral Mass Spectrometer on the lunar atmosphere and Dust Environment Explorer mission. Space Sci Rev 185:27–61
Mahaffy PR et al (2015) The neutral gas and Ion Mass Spectrometer on the Mars atmosphere and Volatile Evolution mission. Space Sci Rev 195:49–73
Mahaffy PR et al (2015) The imprint of atmospheric evolution in the D/H of Hesperian clay minerals on Mars. Science 347:412–414
Mandt KE, Mousis O, Marty B, Cavalie T, Harris W, Hartogh P, Willacy K (2015) Constraints from comets on the formation and volatile acquisition of the planets and satellites. Space Sci Rev 197:297–342
May RD et al (2001) The MVACS tunable diode laser spectrometers. J Geophys Res 106:17673–17682
McKeegan KD et al (2011) The oxygen isotopic composition of the Sun inferred from captured solar wind. Science 332(6037):1528–1532
Miller KE, Theiling B, Hofmann AE, Castillo-Rogez J, Neveu M, Hosseini S, Drouin BJ (2021) The value of CHONS isotopic measurements of major compounds as probes of planetary origin, evolution, and habitability. Bull Am Astron Soc 53(4):243
Mousis O et al (2022) Moonraker: Enceladus Multiple Flyby mission. Planet Sci J 3(12):268
National Academies of Sciences, Engineering, and Medicine (2022) Origins, worlds, and life: a decadal strategy for planetary science and astrobiology 2023-2032. The National Academies Press, Washington
Niemann HB, Harpold DN, Atreya SK, Carignan GR, Hunten DM, Owen TC (1992) Galileo probe mass-spectrometer experiment. Space Sci Rev 60:111–142
Niemann H et al (1997) The Gas Chromatograph Mass Spectrometer aboard Huygens. In: Wilson A (ed) Huygens: science, payload and mission. ESA Special Publication, SP-1177. European Space Agency, Noordwijk, p 85
Niemann HB, Atreya SK, Carignan GR, Donahue TM, Haberman JA, Harpold DN, Hartle RE, Hunten DM, Kasprzak WT, Mahaffy PR, Owen TC, Way SH (1998) The composition of the Jovian atmosphere as determined by the Galileo probe mass spectrometer. J Geophys Res 103:22831–22846
Niemann HB et al (2010) Composition of Titan's lower atmosphere and simple surface volatiles as measured by the Cassini-Huygens probe GCMS experiment. J Geophys Res, Planets 115(E12):E12006. https://doi.org/10.1029/2010JE003659
Owen T, Mahaffy PR, Niemann HB, Atreya S, Wong M (2001) Protosolar nitrogen. Astrophys J 553:L77–L79
Sakamoto N et al (2007) Remnants of the early solar system water enriched in heavy oxygen isotopes. Science 317:231–233
Scott ERD, Krot AN (2001) Oxygen isotopic compositions and origins of calcium-aluminum-rich inclusions and chondrules. Meteorit Planet Sci 36:1307–1319
Sekine Y et al (2014) Exploration of Enceladus' water-rich plumes toward understanding of chemistry and biology of the interior ocean. Trans Jpn Soc Aeronaut Space Sci, Aerosp Technol Jpn 12(ists29):Tk_7–Tk_11
Stern JC et al (2022) Organic carbon concentrations in 3-billion-year-old lacustrine mudstones of Mars. Proc Natl Acad Sci 119(27):e2201139119
Theimens MH (1999) Mass-independent isotope effects in planetary atmospheres and the early solar system. Science 283(5400):341–345
Theimens MH, Lin M (2021) Discoveries of mass independent isotope effects in the solar system: past, present and future. Rev Mineral Geochem 86(1):35–95
Trainer MG et al (2018) Dragonfly: investigating the surface composition of Titan, LPSC, Woodlands, TX
Vasavada AR (2022) Mission overview and scientific contributions from the Mars Science Laboratory Curiosity rover after eight years of surface operations. Space Sci Rev 218:14. https://doi.org/10.1007/s11214-022-00882-7
Waite H et al (2017) Cassini finds molecular hydrogen in the Enceladus plume: evidence for hydrothermal processes. Science 356(6334):155–159
Webster CR (1985) The Brewster-Plate Spoiler: a novel method for reducing the amplitude of interference fringes which limit tunable laser absorption sensitivities. J Opt Soc Am B 2:1464–1470

Webster CR, Heymsfield AJ (2003) Water isotope ratios D/H, $^{18}O/^{16}O$, $^{17}O/^{16}O$ in and out of clouds map dehydration pathways. Science 302:1742–1745

Webster CR, Sander SP, Beer R, May RD, Knollenberg RG, Hunten DM, Ballard J (1990) Tunable diode laser IR spectrometer for in situ measurements of the gas composition and particle size distribution of Titan's atmosphere. Appl Opt 29(7):907–917

Webster CR, May RD, Trimble CA, Chave RG, Kendall J (1994) Aircraft (ER-2) Laser Infrared Absorption Spectrometer (ALIAS) for in-situ stratospheric measurements of HCl, N_2O, CH_4, NO_2, and HNO_3. Appl Opt 33:454–472

Webster CR, Flesch GJ, Haberle R, Bauman J (2004) Mars Laser Hygrometer. Appl Opt 43:4436–4445

Webster CR et al (2013) Isotope ratios of H, C, and O in CO_2 and H_2O of the Martian atmosphere. Science 341:260

Webster CR et al (2021b) Day-night differences in Mars methane suggest nighttime containment at Gale crater. Astron Astrophys 650:A166. https://doi.org/10.1051/0004-6361/202040030

Webster CR, Flesch GJ, Briggs RM, Fradet M, Christensen LE (2021a) Herriott cell spot imaging increases the performance of tunable laser spectrometers. Appl Opt 60(7):1958–1965

Wiechert U et al (2001) Oxygen isotopes and the Moon-forming giant impact. Science 294(5541):345–348

Wong MH et al (2004) Updated Galileo Probe Mass Spectrometer measurements of carbon, oxygen, nitrogen, and sulfur on Jupiter. Icarus 171:153. https://doi.org/10.1016/j.icarus.2004.04.010

Wong MH et al (2013) Isotopes of nitrogen on Mars: atmospheric measurements by Curiosity's mass spectrometer. Geophys Res Lett 40:6033–6037

Wong MH et al (2024) Multiple probe measurements at Uranus motivated by spatial variability. Space Sci Rev 220